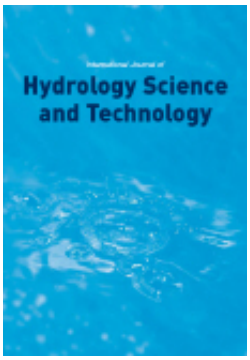

International Journal of Hydrology Science and Technology

ISSN online: 2042-7816 - ISSN print: 2042-7808
https://www.inderscience.com/ijhst

Impact of spatial filtering to GRACE-FO-derived TWS changes: a case study of European river basins

Artur Lenczuk

DOI: 10.1504/IJHST.2025.10072697

Article History:

Received:	18 March 2025
Last revised:	28 May 2025
Accepted:	07 June 2025
Published online:	11 August 2025

Impact of spatial filtering to GRACE-FO-derived TWS changes: a case study of European river basins

Artur Lenczuk

Faculty of Civil Engineering and Geodesy,
Military University of Technology,
Street Gen. Sylwestra Kaliskiego 34, 00-908, Warsaw, Poland
Email: artur.lenczuk@wat.edu.pl

Abstract: Data provided by the gravity recovery and climate experiment (GRACE) and its successor follow-on (-FO) mission are noisy and thus an appropriate spatial filter is required to reliable assessment of the real (geo-)physical signals. This study applies traditional Gaussian smoothing approach and two different data-driven approaches, i.e.: 1) method of scale; 2) method of deviation to study the impact of spatial averaging of GRACE-FO data to leakage and total signal of total water storage (TWS) across major 24 European river basins. The greatest differences between filters are observed in regions indicating divergent TWS signals within small catchments. There are variations in trend values of ±1–2 cm/yr and amplitudes of up to 5 cm in the western and the northeastern European basins. Estimated true leakage represents at least 30% of total TWS signal. Moreover, TWS leakage error is at least 2–3 times larger for original than for both data-driven approaches.

Keywords: GRACE follow-on; total water storage; TWS uncertainty; leakage effect; method of scale; method of deviation; Gaussian smoothing; European river basins; linear trend; (semi-)annual amplitude; least squares estimation; LSE.

Reference to this paper should be made as follows: Lenczuk, A. (2025) 'Impact of spatial filtering to GRACE-FO-derived TWS changes: a case study of European river basins', *Int. J. Hydrology Science and Technology*, Vol. 20, No. 5, pp.1–30.

Biographical notes: Artur Lenczuk is an Assistant Professor at the Military University of Technology in Poland. He is a specialist in gravimetry and physical geodesy. He is working on the application of geodetic measurements to study hydroclimatic and hydrometeorological trends.

1 Introduction

The measurement of the Earth's gravity field has been instrumental in studying and monitoring hydrological processes. These analyses of variations in gravity field offer insights into changes in mass distribution, primarily driven by water storage in various forms and their movement by providing vital information for understanding the water cycle, predicting water resource availability, and addressing challenges like groundwater depletion, or flood and drought risk. These measurements enable to quantify the real changes in terrestrial water storage (TWS) at different temporal resolutions over large

(satellite gravimetry) and local (ground-based and airborne gravimetry) spatial scales (Rodell et al., 2018) that are difficult to accomplish through traditional hydrological monitoring methods (Scanlon et al., 2016).

The satellite gravimetry, such as the gravity recovery and climate experiment (GRACE; Tapley et al., 2004) and its successor, GRACE follow-on (GRACE-FO; Landerer et al., 2020), overcomes many of the ground-based and airborne gravimetry limitations by offering global coverage and the ability to monitor broad-scale hydrological changes (Ince et al., 2019) quantificating TWS changes with unprecedented accuracy and consistency since 2002 (Chen et al., 2022). However, GRACE-derived TWS are subject to various errors arising from various data processing techniques and model integration (Tapley et al., 2004; Chen et al., 2022). In the context of GRACE data processing, different background models are applied to remove large-scale effects, signal corrections and aiding in the separation of hydrological signals from other sources of mass redistribution (Lenczuk et al., 2020). The misinterpretation of GRACE signals are related with errors in implemented background models such as the static gravity field, tidal or non-tidal ocean and atmosphere models or the gradual rebound of the Earth's crust after the melting of ancient ice caps introduced by glacial isostatic adjustment (GIA) model (Chen et al., 2022). The truncation of spherical harmonics or temporal errors such as aliasing lead to the loss of real physical signals resulting in incomplete or distorted representations of dynamic TWS changes (Rodell et al., 2004; Khaki et al., 2018). In the spatial domain, TWS errors may resulting from the limitations of GRACE onboard sensors such as accelerometers and the K-band distance measurement system introducing high-frequency noise into the gravity data (Kim and Lee, 2009). To avoid distortion of TWS estimates, post-processing techniques such as destriping (Swenson and Wahr, 2006), the isotropic Gaussian (Wahr et al., 1998), the time-dynamic (Seo and Wilson, 2005), the decorrelation (Kusche, 2007, Kusche et al., 2009) filters, and the filter depending on the degree and order of the spherical harmonics coefficients (Guo et al., 2010) are used. Albeit all of them involve trade-offs, as excessive smoothing can blur smaller hydrological features.

Both the limited spatial resolution and smoothing required during data processing address leakage effects leading to signal disruption of the analysed area by signals from adjacent areas (Swenson and Wahr, 2002; Long et al., 2015). To address this issue, and improved the accuracy and utility of GRACE-derived TWS estimates, various methods have been developed and refined involving advanced data processing techniques such as forward modelling, post-processing correction, multiplicative approach, optimisation-based filtering, iterative least squares filtering (Ramillien et al., 2005; Klees et al., 2007; Longuevergne et al., 2010; Velicogna et al., 2014; Wiese et al., 2016). For example, Klees et al. (2007) used the adaptive (tailored) filters in preserving signal magnitude and reducing errors for regions with sharp boundaries such as coastlines and river basins. They showed an increase in correlation of at least 0.1 with hydrological models and ground-based observations, and leakage reduction of 10%–20% compared to standard Gaussian filters. The improved correlation of 0.3 between corrected GRACE-derived TWS and Global Land Data Assimilation System (GLDAS) model was indicated by Longuevergne et al. (2010) for the high plains aquifer. They estimated leakage correction based on the multiplicative factor approach restored attenuated signals, reducing the GRACE error by a factor of ~10. Watkins et al. (2015) and Save et al. (2016) proposed the use of spherical cap mass concentration elements (mascons, MSCs), while relying on external information provided by near-global geophysical

models to constrain the solution. Wiese et al. (2016) developed an optimised coastline resolution improvement (CRI) regional filter that reduced leakage errors for mascons. They reveal a reduction in leakage errors of ~50%, indicating averaged globally residuals near ~1 cm equivalent water height (EWH).

However, most of previous studies examining both spherical harmonics and mascons to pass signal and reject noise uses a priori water storage estimates from complementary datasets, including precipitation records, soil moisture data, and outputs from hydrological models and scaling approach (Landerer and Swenson, 2012; Long et al., 2015). However, models vary spatially and temporally, and are burdened with errors in their inputs (Döll et al., 2012, 2014; Schmied et al., 2021; Lenczuk et al., 2020). Hydrological model calibration errors can skew the leakage corrections or over-smooth GRACE data, suppressing natural variability or sharp gradients in mass changes introducing further uncertainties to the obtained results, especially in regions undergoing rapid hydrological or climatic changes (Scanlon et al., 2018). For example, Vishwakarma et al. (2016) have already shown that the phase changes can take up to one month and may make difficult for users to recover the signal by scaling alone leading to, among others, amplitude loss in time series of the analysed Earth's gravity field parameters.

In this research, to assess the magnitude of leakage effect of TWS signal the traditional Gaussian smoothing and two different data-driven approaches, i.e., method of scale and method of deviation proposed by Vishwakarma et al. (2016, 2017) are used. In contrast to previous studies, the filtered GRACE-FO gravity fields only are implemented; no external data will be included in the analyses. GRACE-FO monthly gravity fields are provided in spherical harmonics form up to degree and order 96. To assess the reliability of TWS changes over 24 European river basins, the Jet Propulsion Laboratory (JPL) GRACE-FO mascon solution and GLDAS hydrological model are employed. This paper makes a fourfold contribution to hydrology and climate science. To the best of my knowledge:

1 There is still no assessment of the impact of GRACE leakage effect on inter-annual and semi-annual.

2 Secondly, this study is the first to identify the contribution of true leakage to total signal over Europe.

3 This study is also the first to assess TWS uncertainty for European river basins.

4 The detailed study the temporal changes of total TWS and true leakage TWS signals for the Rhone, Neman and Vuoksi-Neva river basin regions for various data filtering approaches are also presented.

The obtained results highlights strong temporal coherence of monthly TWS changes derived from GRACE-FO spherical harmonic coefficients (SHCs) and mascon, and hydrological model during drought and flood events recorded in European areas. However, the magnitude of TWS changes is different.

The article is arranged as follows: in Section 2, the used data such as GRACE-FO gravimetric mission data, GLDAS hydrological model, and assumed methodology are described. Section 3 presents the study area. An overview of the results and a detailed discussion are presented in Section 4. Then, the article is completed with conclusions in Section 5. This article explores the quality of gravity field measurements and assessment of signal leakage for their application in hydrological studies. By examining the current

state of gravity-based research, the paper aims to provide a comprehensive analysis of GRACE-FO data filtered by various methods to understand method selection for contributions to hydrological research and forecasting of extreme phenomena such as droughts and floods, which can be helpful to decision makers.

2 Data and methodology

2.1 GRACE-FO monthly solutions

This research bases on the newest Level-2 release (RL) 06.3 GRACE-FO data in the form of SHCs up to degree and order (d/o) 96, which are provided by three science data systems (SDSs), i.e., the Center Space Research (CSR) at Austin (Save, 2024), the German Research Center for Geosciences (GFZ) at Potsdam (Dahle, 2024) and JPL at Pasadena (McCullough et al., 2024). All GRACE-FO data are free available at https://icgem.gfz-potsdam.de/home. GRACE-FO data are pre-processed replacing low-degree coefficient: degree-1 coefficients estimated using the method of Sun et al. (2016) from technical note (TN)-14 and TN-13a, 13b, 13c, respectively for CSR, GFZ and JPL. C30 and C20 coefficients by independent estimates from satellite laser ranging (SLR) (Loomis et al., 2020).

All low-degrees corrections are available at https://podaactools.jpl.nasa.gov/. The post glacial rebound effects are removed using the ICE6G-D model from Peltier et al. (2018). Finally, I analyse over five-years (67 monthly) data for June 2018 to February 2024. The presented TWS results are estimated in the form of the anomalies relative to GGM05C static gravity field model (Ries et al., 2016).

2.2 Reliability of the obtained results

To assess the reliability of results GRACE-FO data provided by JPL processing centre as gridded TWS anomalies (Watkins et al., 2015) are applied. TWS RL06.1_v03 mascons are presented on a grid 0.5° per 0.5° in form of mascon. Mascons are mass concentration blocks defined within the range between 89.75°N to 89.75°S for latitude and within the range of 0.25° to 359.75°E for longitude. Mascons are placed on the surface of an elliptical Earth, i.e., the *ellipsoidal corrections* that are necessary to interpret spherical harmonic solutions are already implemented during the processing (Li et al., 2017). TWS anomalies are estimated relative to the 2004.0–2009.999 baseline. They are less affected by leakage errors than SHCs, do not require empirical filters to remove north-south strips and have greater correlation with in situ data as well (Watkins et al., 2015). More detailed information about the JPL mascon processing can be found at https://grace.jpl.nasa.gov/data/get-data/jpl_global_mascons/. Finally, 67 GRACE-FO monthly data since June 2018 are implemented. Further, this study compares GRACE-FO-derived TWS SHC with TWS changes calculated as a sum of plant canopy water storage, snow water storage and soil moisture components provided in GLDAS Noah hydrological model (Rodell and Beaudoing, 2003). GLDAS water changes are available from January 1979 until the present and are defined on a global grid of 0.25° per 0.25°. Monthly GLDAS TWS since June 2018 until February 2024 are applied to be consistent with analysed GRACE-FO period.

2.3 Methodology

To reduce noise included in GRACE-FO data, isotropic Gaussian smoothing (Wahr et al., 1998) are used. It depends on the position of the kernel and the maximum degree and order of SHCs. The averaging function (W) is described in equation (59) of Jekeli (1981) publication as follow:

$$W_0 = \frac{1}{2\pi}, W_1 = \frac{1}{2\pi}\left[\frac{1+e^{-2b}}{1-e^{-2b}} - \frac{1}{b}\right], W_{n+1} = -\frac{2n+1}{b}W_n + W_{n-1} \tag{1}$$

with:

$$b = \frac{\ln(2)}{\left(1-\cos\left(\frac{r}{a}\right)\right)},$$

where n mean a maximum degree of SHCs, r is a filter radius, b stands for a dimensionless parameter characterising the smoothing process and a mean a radius of Earth. Next, two another filters, i.e., method of scale (Vishwakarma et al., 2016), and method of deviation (Vishwakarma et al., 2017) are applied. They are data-driven approaches based only on GRACE-FO-filtered fields. These methods enable estimating the magnitude of true leakage signal from individual river basins area as well as corrected TWS series for GRACE-FO data. In the case of method of scale, the scale factor is estimated using uniform layer approximation. Scale factor depends on the implemented filter kernel and the basin mask, i.e., shape and size of basin, and is used to counter the attenuation of the basin-confined signal. To detail, method rely on determining the signal leakage $(\widehat{f_c})$ based only on filtered gravity field using formula:

$$\widehat{f_c} = s\left(\overline{g_c} - \widehat{l_c}\right), \tag{2}$$

where $\overline{g_c}$ is the filtered GRACE type gravity field, $\widehat{l_c}$ and s mean the estimated leakage and scale factor, respectively. Here, the north-south stripes are reduced using the isotropic Gaussian filter with 400 km radius. Finally, the leakage and its magnitude is calculated using (Vishwakarma et al., 2016):

$$f_c = s\left(\overline{f_c} - \widehat{l_c}\right), \tag{3}$$

where $\overline{f_c}$ is the regional average of the filtered field.

In the case of estimating and restoring the suppressed geophysical signal due to filtering, this study uses a fairly new data-based method that is able to correct the signal loss independent of the catchment size, i.e., method of deviation. In this method, in order to calculate the deviation field, the first step is to estimate the regional average for a given area, and then to remove it from field limited to analysed area. Then, filtering the designated deviation field and calculating the regional average allow to obtain the deviation integral. Thus, finally the regional average f_c for the area c of the field $f(\theta, \lambda)$ can be written as (Swenson, 2002):

$$f_c = \frac{1}{A_c}\int_{\Omega} f(\theta\ \lambda)R(\theta\ \lambda)d\Omega, \tag{4}$$

where A_c is the area, $R(\theta, \lambda)$ is the area characteristic function: 1 inside and 0 outside, Ω is the domain of the surface of the Earth and $d\Omega$ is the infinitesimal surface element $\sin\theta d\theta d\lambda$. After few computational procedures (Vishwakarma et al., 2017), the true regional average f_c is saved as:

$$f_c = \overline{f_c} - \overline{SF_c} - l_c, \tag{5}$$

where $\overline{SF_c} = \frac{1}{A_c}\int_{\Omega} \overline{SF}(\theta, \lambda)R(\theta, \lambda)d\Omega$ and l_c means true leakage. It worth to notice that it further attempts to obtain the deviation integral for method of deviation, which is determined from the filtered deviation field and the regional average estimated for the selected area. Consequently, the restored signal is independent of river basin size. To find more information about data-driven method of deviation the readers are referred to Vishwakarma et al. (2017) study.

2.4 Study of the results quality

To assess the quality of signal leakage and estimating its contribution to total TWS signal, three metrics: the component contribution ratio (*CCR*), the initial leakage error ($ERR_{leakage}$), and the root-mean-square (RMS) reduction (RMS_{red}) are calculated. Firstly, to study the importance of true leakage [equations (1)–(4)] to the total TWS time series, CCR values (Kim et al., 2009) are estimated following:

$$CCR = \frac{1}{N}\sum_{t=1}^{N}\frac{MAD}{TWS_t}, \tag{6}$$

where *MAD* is the median absolute deviation calculated as $MAD = \frac{1}{N}\sum_{t}^{N}\left|LEAK_t - \overline{LEAK}\right|$, N means the number of t-months for individual TWS time series. $LEAK_t$ stands for the leakage signal of TWS estimated for individual river basin and $\overline{LEAK}$ is mean of GRACE-FO-derived TWS from each CSR, GFZ, JPL processing centre. Further, to intercomparing of various filtering approaches for GRACE-FO data and quantify the difference of leakage signal using each approach, the initial GRACE-FO TWS leakage error due to used three filtering approach ($ERR_{leakage}$; Tripathi et al., 2022) are computed over European regions. It is estimated using following formula:

$$ERR_{leakage} = std\left(TWS_t^{unf} - TWS_t^{f}\right)\cdot\frac{RMS\left(TWS_t^{MSC}\right)}{RMS\left(TWS_t^{f}\right)}, \tag{7}$$

where TWS_t^{unf} is the unfiltered GRACE-FO TWS signal for the t^{th} month. ΔTWS_t^{f} represents the filtered TWS using Gaussian smoothing and using two data-driven approaches. TWS_t^{MSC} is TWS changes estimated for GRACE-FO JPL mascon solution. t is a number of observations (months) for time series (it worth to noticed that this is relevant for comparing various filtering schemes, but not providing a true estimate of

leakage error). Finally, to investigate impact of the filter selection causing the differences on the final signal, the reduction in temporal RMS (RMS_{red}) is computed after subtracting the common filtering approach (Gaussian smoothing with radius equal to 400 km ('original'); TWS^{fG}) from data-driven (TWS^{fdm}), i.e., method of scale ('m. of scale') and method of deviation ('m. of deviation'). The relative reduction in RMS value is determined as signal variability of $RMS(TWS^{fdm})$ and the variability of reduced TWS masses ($RMS(TWS^{fdm} - TWS^{fG})$ as follows:

$$RMS_{red} = \frac{RMS\left(TWS^{fdm}\right) - RMS\left(TWS^{fdm} - TWS^{fG}\right)}{RMS\left(TWS^{fdm}\right)} \cdot 100. \tag{8}$$

Figure 1 The major 24 European river basins selected using the UN Global Compact initiative (see online version for colours)

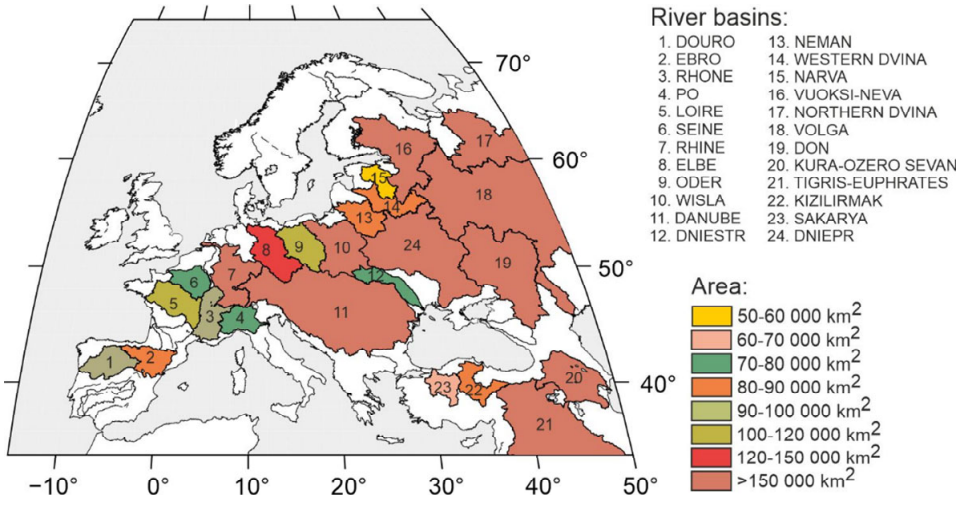

3 Study area

In the last few years, since the launch of GRACE-FO mission, Europe experienced more frequent and severe dry and wet events, indicating warning conditions (European Drought Observatory, 2018; Bevacqua et al., 2024; Knutzen et al., 2025). Already in 2018, the decreases in precipitation were recorded, combining with summer heat wave to lead to exceptional drought in Central Europe (Toreti et al., 2019). Further June-July 2019 heat waves and below-average precipitation led to other severe drought in the following two years (European Drought Observatory, 2019; Rakovec et al., 2022). In 2020, periodic torrential rains triggered flash floods across Europe, affecting western and southern parts. A series of summer storms and severe weather resulted in significant rainfall led to next floods in western Europe throughout 2021 (Lehmkuhl et al., 2022). In summer 2022, southern regions of Europe experienced exceptionally pronounced atmospheric and soil dryness caused by a sequence of heatwaves and acute lack of rainfall (Bevacqua et al., 2024) (Table A1). These events have reduced municipal water supplies, crop yields, decreased hydropower generation, restricted navigation in rivers,

compromised stability of dykes and intensified the wildfires in Europe (Kapica et al., 2024), which is getting challenged in hydro-meteorological and-climatic studies (Rakovec et al., 2022). Hence, this study focuses on the major European river basins using datasets from the United Nations (UN) Global Compact initiative. Only catchments experienced by extreme hydrometeorological changes in recent years and characterised by areas of at least 50 000 km^2, e.g., the Narva basin are considered (Table A1). That way, 24 river basins are analysed, the largest selected catchments of which have more than 150,000 km^2, i.e., the Rhine (7), Danube (11), Vuoksi-Neva (16), Northern Dvina (17), Volga (18), Don (19), Kura-Ozero Sevan (20), Tigris-Euphrates (21) and Dniepr (24) (Figure 1).

4 Results and discussion

4.1 Spatial analysis: intra-and annual signals

This study focuses on analysis of long-term (Figure 2) and (semi-)annual (Figure 3 and Figure 4) TWS signal determined from GRACE-FO SHCs spatially averaged using Gaussian smoothing with 400 km radii ('original' approach) and TWS signal determined from gravity field filtered using method of scale ('m. of scale') and method of deviation ('m. of deviation'). The values are estimated using the least squares estimation (LSE) method. Firstly, the effect of spatial filtering used on average values of linear trend computed for selected 24 European river basins (Figure 2) are analysed. A similar spatial distribution of trend signs for all approaches is noted. Positive trends dominate in the northern and northeastern catchments, however, negative values are found in the southern and western regions. The largest differences in trend signs are found over central Europe between three GRACE-FO SDS solutions. For original approach, change in trend signs for the Rhine, Wisla and Volga basins is observed. For both data-driven approaches differences are noticeable for the Wisla, Elbe, Western Dvina, Volga, Kizilirmak, and extra Danube for method of scale. There are changes in trend of ±1–2 cm/yr for the data-based fields compared to original fields. The largest trends above 5 cm/yr are found for the Narva, Vuoksi-Neva, and the smallest trends below –4 cm/yr for the Rhone, Sakarya for all datasets. The largest values are noted for GFZ SHCs for the Vuoksi-Neva basin equal to 4.1 cm/yr, 10.4 cm/yr and 7.9 cm/yr respectively for original, method of scale and method of deviation approaches. The obtained high positive TWS trends in northern regions coincide with increasing precipitation. The values are consistent with the prediction of Intergovernmental Panel on Climate Change (IPCC) models (Rodell et al., 2018). On the other hand, the lowest values are noticed for Sakarya. Trends around –3.5 cm/yr are observed for original data for GFZ SHCs and JPL SHCs, and –10 cm/yr for GFZ SHCs for both data-driven filtering approaches (Table A2). The evident significant decline in water resources within Turkish river basins reflects groundwater extraction (Xanke and Liesch, 2022), caused by the prevailing temperate climate with dry summers and winters. In comparison to mascon solution, data-driven approaches reveal the extreme trends more effectively. The differences of trend sign between mascon and SHCs are noted for the coastal areas of Western Europe, i.e., the Loire, Seine, Rhine and Kizilirmak basins located in Turkey. It is probably due to still existing and stronger ocean-land leakage in SHCs data (the constraints are more rigorous for mascons, given the geometric and physical constraints used in their construction). In the case of JPL

MSC, the leakage is reduced by the CRI method (Watkins et al., 2015). For GLDAS, trend are underestimated, however, positive values still dominate in the northern and eastern parts of Europe and negative values occur in southern and western regions, i.e., the Douro, Ebro, Loire, Tigris-Euphrates basins.

Figure 2 Maps of the linear trend (cm/yr) estimated within European river basins for average TWS changes (see online version for colours)

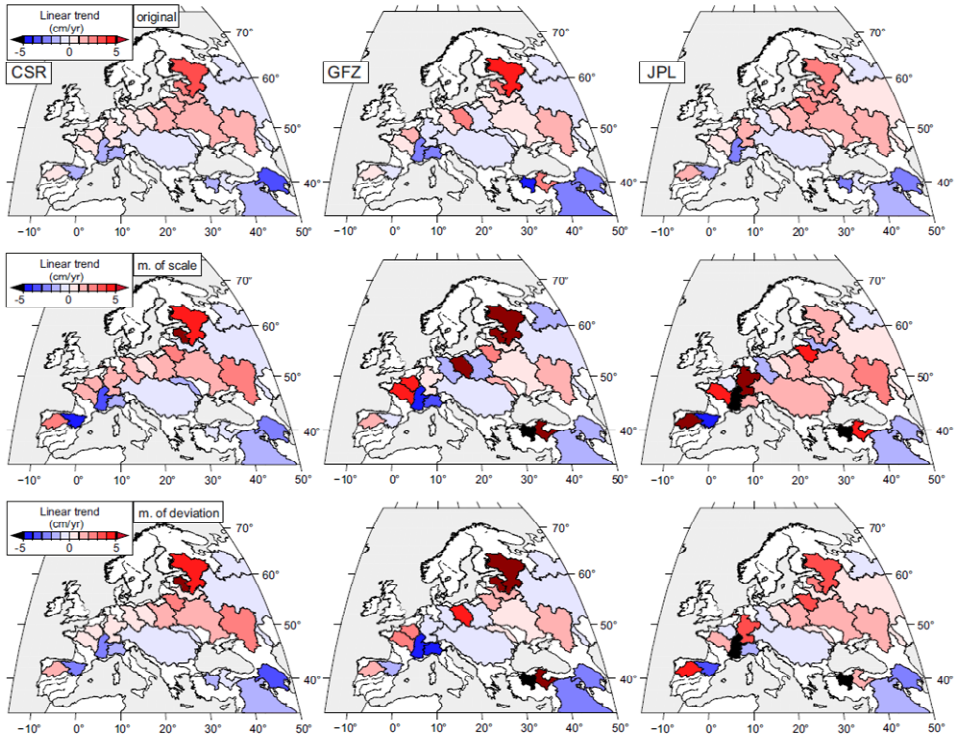

Notes: TWS are estimated using original GRACE-FO SHCs up to degree and order 96 provided by CSR, GFZ and JPL processing centres (from left to right columns). GRACE-FO signals are filtered with Gaussian smoothing with radius equal to 400 km (top) and using two data-driven approaches, i.e., method of scale (middle) and method of deviation (bottom rows).

In case of amplitude of annual oscillation, values above 5 cm dominate for most regions (Figure 3). The values decrease from east and west to central part of Europe for all three filtering approaches and all processing data centres. There are amplitudes around 3 cm or lower for original fields for the Western Diva, Vuoksi-Neva river basins for CSR SHCs and for the Po, Dniester, Neman, Narva, Kura-Ozero Sevan basins for GFZ SHCs, with the Neman characterised by the smallest value of 1.1 cm. For JPL SHCs, amplitudes are above 4 cm. For both data-driven approaches, amplitude are at least 1.5-to 2-times larger than values for original approach. The extreme amplitudes are obtained for the Narva for CSR SHCs, the Seine, Vuoksi-Neva, Sakarya for GFZ SHCs, the Ebro, Vuoksi-Neva, Tigris-Euphrates for JPL SHCs for method of scale. In the case of method of deviation, the extreme values are found for the Rhone, Sakarya for CSR SHCs and the Seine, Sakarya for GFZ SHCs. All of them are characterised with amplitudes over 10 cm for

three filtering methods. Overall, there is a spatial coherence for all SHCs. However, GFZ SHCs amplitudes for the Ebro, Elbe, Neman, Vuoksi-Neva basins are overestimated compared to others. The prominent seasonal changes in the north(-east)ern and western regions are caused by strong interannual variations in precipitation (Barton et al., 2022), however, the maximum values in the southern regions are the result of strong temperature anomalies between summer and winter periods (European State of the Climate, 2021). For mascon solutions and GLDAS model, the spatial pattern of maximum values is overlap with GRACE SHCs approach. The greatest values are found in the east-west belt along the Baltic coast and also for river basins of Turkey. The smallest values are observed across Central Europe. However, compared to all GRACE-FO approaches, the amplitudes are overestimated by 3–5 cm on average for GLDAS, especially for western regions (Figure 6).

Figure 3 Maps of the amplitude of the annual oscillation (cm) estimated within European river basins for average TWS changes (see online version for colours)

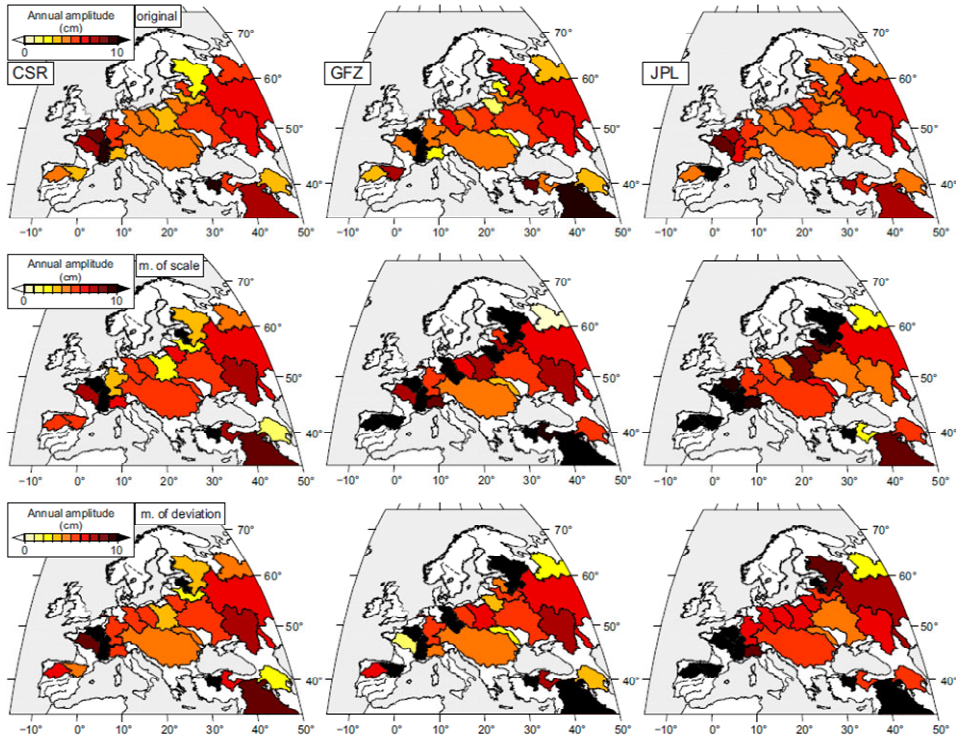

Notes: TWS are estimated using original GRACE-FO SHCs up to degree and order 96 provided by CSR, GFZ and JPL processing centres (from left to right columns). GRACE-FO signals are filtered with Gaussian smoothing with radius equal to 400 km (top) and using two data-driven approaches, i.e., method of scale (middle) and method of deviation (bottom rows).

The spatial pattern of semi-annual amplitude (Figure 4) is coherent with annual amplitude (Figure 3). The maximum values are observed for west and north parts of Europe, especially for the Baltic Sea regions. The obtained values are mainly comparable for all GRACE-FO data and filtering methods, excluding method of scale for which the values

are overestimated for GFZ SHCs. The largest amplitudes over 4 cm are found for the Ebro, Rhone, Loire, Elbe, Narva, Vuoksi-Neva basins for original approach and additionally the Douro, Kizilirmak, Sakarya for method of deviation, and mostly basins located in west, north and south parts of Europe for method of scale. The values obtained for the Rhine, Wisla, Neman, Western Dvina river basins are overestimated for GFZ SHCs data-driven approaches compared to CSR SHCs and JPL SHCs. A comparison of obtained SHC results with mascon and hydrological model reveals a similar spatial distribution of semi-annual amplitudes for all GRACE-FO data. The maximum values occur in the northern and western European river basins for mascon and GLDAS; values are presented in Table A4. GLDAS overestimates semi-annual mostly for eastern areas. The greatest consistency of results with reference datasets are observed for CSR SHCs, however, amplitudes are overestimated for GFZ SHCs.

Figure 4 Maps of the amplitude of the semi-annual oscillation (cm) estimated within European river basins for average TWS changes (see online version for colours)

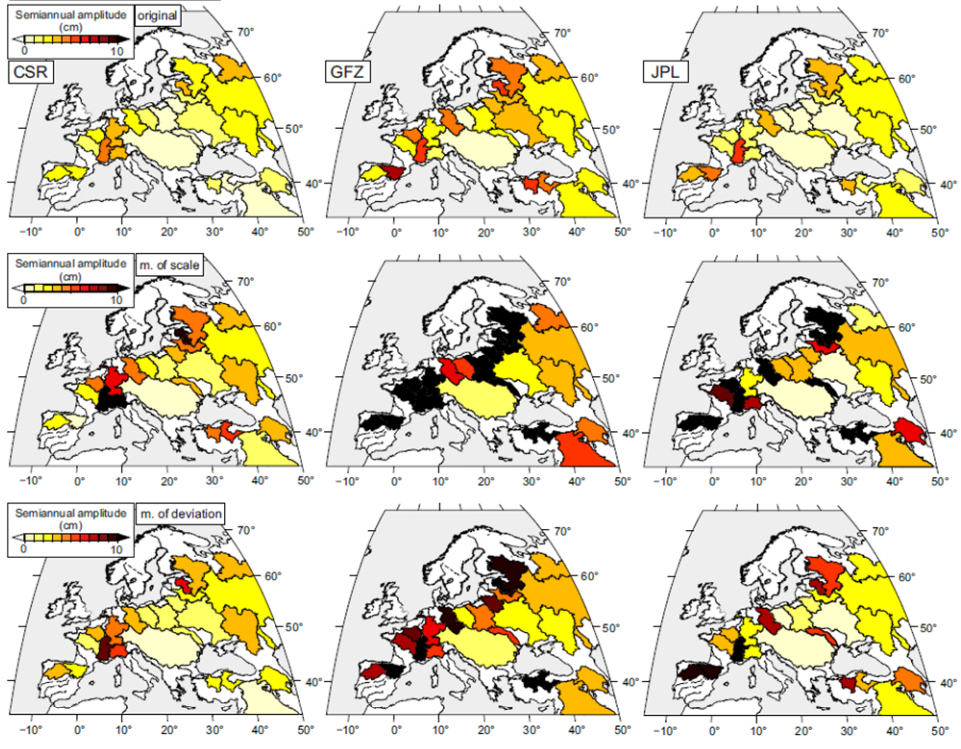

Notes: TWS are estimated using original GRACE-FO SHCs up to degree and order 96 provided by CSR, GFZ and JPL processing centres (from left to right columns). GRACE-FO signals are filtered with Gaussian smoothing with radius equal to 400 km (top) and using two data-driven approaches, i.e., method of scale (middle) and method of deviation (bottom rows).

In the case of RMS, CSR SHCs and JPL SHCs original approaches are mostly characterised with values smaller than 30 cm, excluding JPL SHCs filtered by method of scale (Figure 5). For basins of northeastern Europe, especially for the Vuoksi-Neva, Northern Dvina and Don basins, RMS for GFZ SHCs are overestimated and are

three-times greater than others. For the method of scale, there is RMS greater than 30 cm for the west to east seacoast belt for all GRACE-FO datasets, excluding river basins of Central Europe for CSR SHCs. RMS magnitudes are comparable with CSR SHCs and JPL SHCs mainly over western Europe basins (Spain, France) and the Baltic areas, for which the largest deviations of TWS exceeding 70 cm for GFZ SHCs for all filtering methods. It is effect of the strong signal leakage effect between ocean and land, which is observed throughout western and central Europe. This has also been noted by Eicker et al. (2020) as a strong negative correlation between daily changes derived from GRACE and the fifth generation ECMWF (European Centre for Medium-range Weather Forecasts) atmospheric reanalysis (ERA5) model. Further, the results obtained for method of deviation highlight that RMS values for the Rhine, Elbe, Oder, Wisla basins are overestimated for all GFZ SHCs approaches and JPL SHCs filtered by method of scale. The strongest spatial agreement with mascons as well as RMS magnitude is found for CSR SHCs and JPL SHCs filtered by original and method of deviation approaches (Figure 6 and Table A5). The values for method of deviation are several cm larger than for original SHCs for Central Europe as well as mascons. For GLDAS, the values are overestimated for all basins indicating RMS greater than 40 cm; however, there are also noticeably smaller values for central basins relative to basins located at the edge of Europe.

Analysis of results for all estimated parameters (Figures 2–6 and Tables A2–A5), there are major differences between original and both data-driven approaches occur in regions of signal leakage are the strongest, i.e., river basins with an area of less than 100,000 km^2. They are located on the belt coasts near the North Sea and Baltic Sea, and river basins located in Turkey. The smallest variations in parameter' values and magnitude are found in the central part of Europe. To better quantify the resemblance of obtained parameters for various spatial filtering methods, values of linear trend, annual and semi-annual amplitudes and RMS relationships for original versus method of deviation for all data processing centres and original versus mascon solution for JPL (Figure 7) are compared. The results are consistent for three selected filtering methods. The greatest divergences are observed for the Narva, Vuoksi-Neva and Kizilirmak for CSR SHCs and JPL SHCs, and the Ebro, Rhone for GFZ SHCs. Annual amplitudes are mainly in range of 3-7 cm for all GRACE-FO processing centres and are larger for method of deviation than original approach. However, semi-annual amplitudes are underestimated for JPL SHCs original approach for 50% of basins compared to method of deviation for CSR SHCs and GFZ SHCs, and JPL mascon solution. CSR SHCs and GFZ SHCs indicate higher fluctuations in RMS for method of deviation than for original and mascon approaches. These are affected by strong semi-annual signals underestimated by JPL SHCs (Figure 4).

4.2 True leakage signals

This study also assesses the contribution of true leakage to total GRACE-FO TWS signal (Figure 8). The spatial distribution of *CCR* is cohesive for all three filtering methods and data processing centres. The highest values are noticed for the northern river basins located in a belt along the continental coast, for which leakage represents mainly at least 30% of total TWS signal, especially for original approach. For most river basins, both data-driven approaches show less leakage than for original. The lowest leakage for Central Europe is observed. The reduction in leakage is most obvious in small river

basins such as the Rhone, Po, Elbe, Neman, Narva, Kizilirmak and Sakarya as well. Furthermore, GFZ SHCs is characterised with higher CCR values than CSR SHCs and JPL SHCs. For original approach, the Loire, Dniester, Kura-Ozero Sevan and Kizilirmak show *CCR* of at least 0.3. The values less than 0.1 are found for the Douro, Seine, Vuoksi-Neva for CSR SHCs, the Volga for GFZ SHCs, and the Vuoksi-Neva for JPL SHCs. For method of scale, only 9, 12 and 5 river basins show *CCR* greater than 0.3 respectively for CSR SHCs, GFZ SHCs and JPL SHCs. The largest values for Rhine (0.82), Ebro (0.55) and Northern Dvina (0.63) for each processing centres are found. In the case of method of deviation, this study notices extreme *CCR* values between 0.3 and 0.6 for all centres, excepting the Western and Northern Dvina river basins for JPL SHCs; values over 0.7.

Figure 5 Maps of the RMS (cm) estimated within European river basins for average TWS changes (see online version for colours)

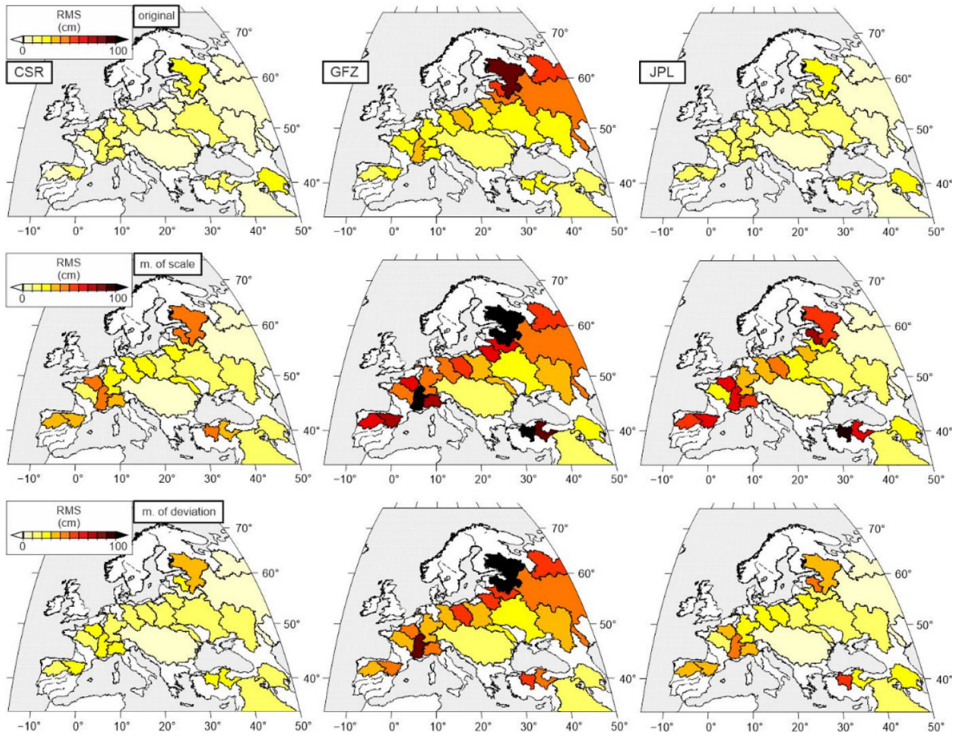

Note: TWS are estimated using original GRACE-FO SHCs up to degree and order 96 provided by CSR, GFZ and JPL processing centres (from left to right columns). GRACE-FO signals are filtered with Gaussian smoothing with radius equal to 400 km (top) and using two data-driven approaches, i.e., method of scale (middle) and method of deviation (bottom rows).

Figure 6 Maps of the linear trend (cm/yr), the amplitude of the annual oscillation (cm) and the RMS (cm) (from left to right columns) estimated within European river basins for average TWS changes derived for GRACE-FO JPL mascon solution (top row) and GLDAS hydrological model (bottom row) (see online version for colours)

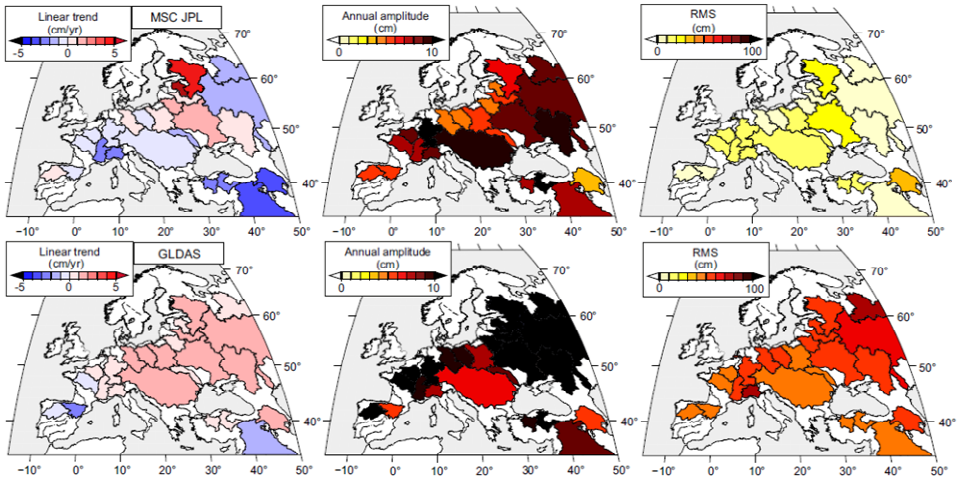

Figure 7 Respective scatter plots of linear trend (cm/yr), amplitude of the annual and semi-annual oscillation (cm) and RMS over 24 European river basins estimated using original Gaussian smoothing with radius equal to 400 km versus the method of deviation approach and mascon solution during the GRACE-FO period (see online version for colours)

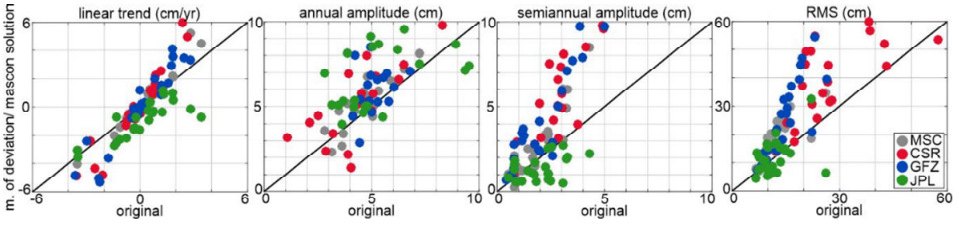

Notes: The black line indicates the 1:1 ratio. The coloured dots indicate data provided by various GRACE-FO processing centres. Noted that mascon solution is compared with JPL original approach.

4.3 Assessment of TWS uncertainty

To quantify TWS uncertainty resulting from leakage effect and spatial averaging of GRACE-FO data over European river basins, two various parameters: TWS leakage error ($ERR_{leakage}$) and RMS reduction (RMS_{red}) are used. Firstly, the magnitudes of TWS leakage error for all three filtering methods are compared. There are the largest values for original approach for all river basins, as well as the maximum values above 40 cm for all filtering method and data processing centres for basins located in the western (the Rhone, Po, Seine and Rhine), northeastern (the Dniester, Neman, Narva) and southern (the Kura-Ozero Seven, Tigris-Euphrates, Kizilirmak and Sakarya) parts of Europe. Regions characterised with leakage error at least 2–3 times larger for original approach than for

both data-driven ones. The lowest values are found for CSR SHCs. Method of scale shows the smallest errors for all GRACE-FO data across Europe, not exceeding 15% of total TWS signal derived for analysed river basins. The comparable values are observed for method of deviation for Eastern Europe. The predominant contribution of leakage error to total TWS signal are noted in the southern regions for GFZ SHCs and JPL SHCs filtered by original and data-driven methods. Regions also characterised with TWS leakage error greater than 100 cm triggered by signals from the Mediterranean Sea and the Black Sea areas.

Figure 8 Maps of the CCR (unitless) of true TWS leakage signal to total variability of TWS estimated within European river basins (see online version for colours)

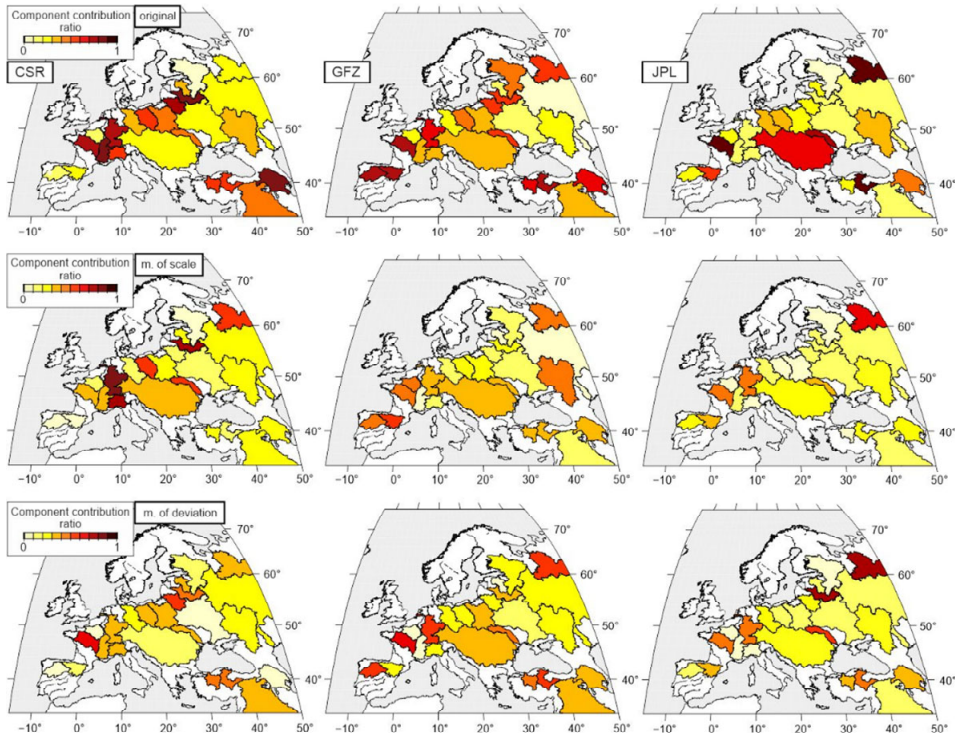

Notes: TWS are estimated using original GRACE-FO SHCs up to degree and order 96 provided by CSR, GFZ and JPL processing centres (from left to right columns). GRACE-FO signals are filtered with Gaussian smoothing with radius equal to 400 km (top) and using two data-driven approaches, i.e., method of scale (middle) and method of deviation (bottom rows).

Further, RMS reduction for 24 European river basins (Figure 10) is calculated to evaluate how strongly a given signal is dampened through the filtering process using different kinds of filters. The parameter is defined by comparing the signal of data-driven approaches with a Gaussian smoothing one [equation (8)]. Figure 10 shows reductions of mostly 30%–50% for all three GRACE-FO datasets using data-driven approaches compared to original one. The largest signal reductions are found adapting method of deviation for CSR SHCs and GFZ SHCs for all river basins, however, method of scale for JPL SHCs. There are values over 70% for both data-driven approaches and for all

SDS GRACE-FO centres for the Wisla, Danube, Dniester, Northern Dvina, Volga and Don basins. These regions are mainly characterised with small interannual changes (central parts) as well as for which the largest signal variance is observed (western parts of Europe). However, minimum values around 10%–20% are noticed for river basins located in the western, northeastern and southern parts of Europe that cover an area smaller than 120,000 km^2.

Figure 9 TWS leakage error (cm) estimated within European river basins (see online version for colours)

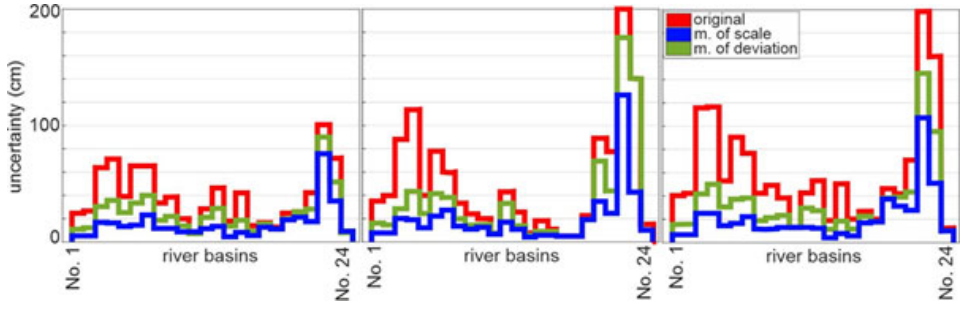

Notes: TWS are estimated using GRACE-FO SHCs up to degree and order 96 provided by CSR, GFZ and JPL processing centres (from left to right columns). GRACE-FO signals are filtered with Gaussian smoothing with radius equal to 400 km ('original') and using two data-driven approaches, i.e., method of scale ('m. of scale') and method of deviation ('m. of deviation'). Noted that this is relevant for comparing three filtering schemes used, but not providing a true estimate of leakage error.

Figure 10 RMS reduction (%) of TWS estimated between GRACE-FO signals are filtered with Gaussian smoothing with radius equal to 400 km and two data-driven approaches, i.e., method of scale (blue curves) and method of deviation (green curves) over European river basins (see online version for colours)

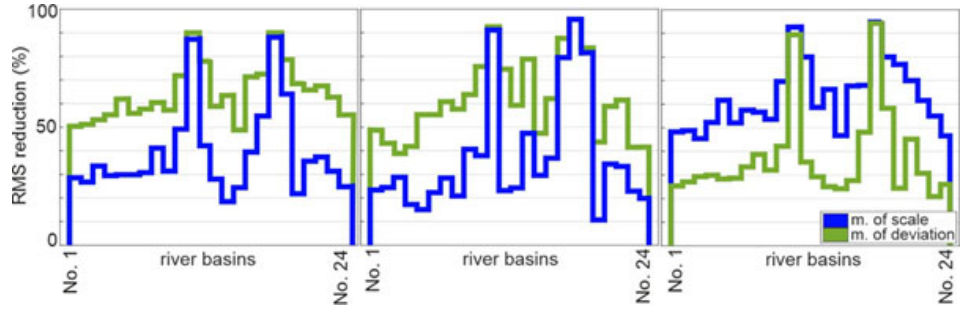

Note: TWS are estimated using original GRACE-FO SHCs up to degree and order 96 provided by CSR, GFZ and JPL processing centres (from left to right columns).

Table 1 The correlation coefficients estimated for Rhone, Neman and Vuoksi-Neva river basins for average GRACE-FO TWS changes derived for SHC provided by CSR, GFZ, JPL and JPL mascon solution

	River basin	*CSR*			*GFZ*			*JPL*		
		Original	*Method of scale*	*Method of deviation*	*Original*	*Method of scale*	*Method of deviation*	*Original*	*Method of scale*	*Method of deviation*
MSC	Rhone	0.87	0.80	*0.92*	0.85	0.79	*0.89*	0.85	0.82	*0.93*
JPL	Neman	*0.91*	0.71	0.89	*0.88*	0.73	0.87	*0.94*	0.77	0.91
	Vuoksi-Neva	*0.89*	0.87	0.86	0.88	0.88	*0.90*	0.92	*0.93*	0.89
GLDAS	Rhone	*0.67*	0.60	0.65	*0.62*	0.59	0.59	0.55	*0.57*	0.48
	Neman	*0.82*	0.75	0.81	*0.78*	0.66	0.64	*0.74*	0.72	0.69
	Vuoksi-Neva	*0.59*	0.52	0.46	*0.53*	0.49	0.42	*0.55*	0.50	0.47

Note: GRACE-FO SHC signals are up to degree and order 96, and are filtered with Gaussian smoothing with radius equal to 400 km (original) and using two data-driven approaches, i.e., method of scale and method of deviation.

4.4 Temporal analysis: river basins

As a next step, this study focuses on estimating the temporal coherence of monthly TWS changes derived for GRACE-FO SHCs and mascon, and hydrological model during recorded periods of drought and flooding in European river basins (Figure 11). It aims to quantify the impact of the chosen filtering method on final TWS signal determined for a period of almost six years. The true leakage and its magnitude (red curves) are also determined. For detailed analysis, three regions:

1 the Rhone

2 Neman

3 Vuoksi-Neva river basins are selected.

Figure 11 Time series of TWS derived for the Rhone (top), Neman (middle) and Vuoksi-Neva (bottom row) river basins for original CSR GRACE-FO filtered using Gaussian smoothing with radii equal to 400 km approach and for gravity fields filtered using two data-driven approaches, i.e., method of scale and method of deviation (see online version for colours)

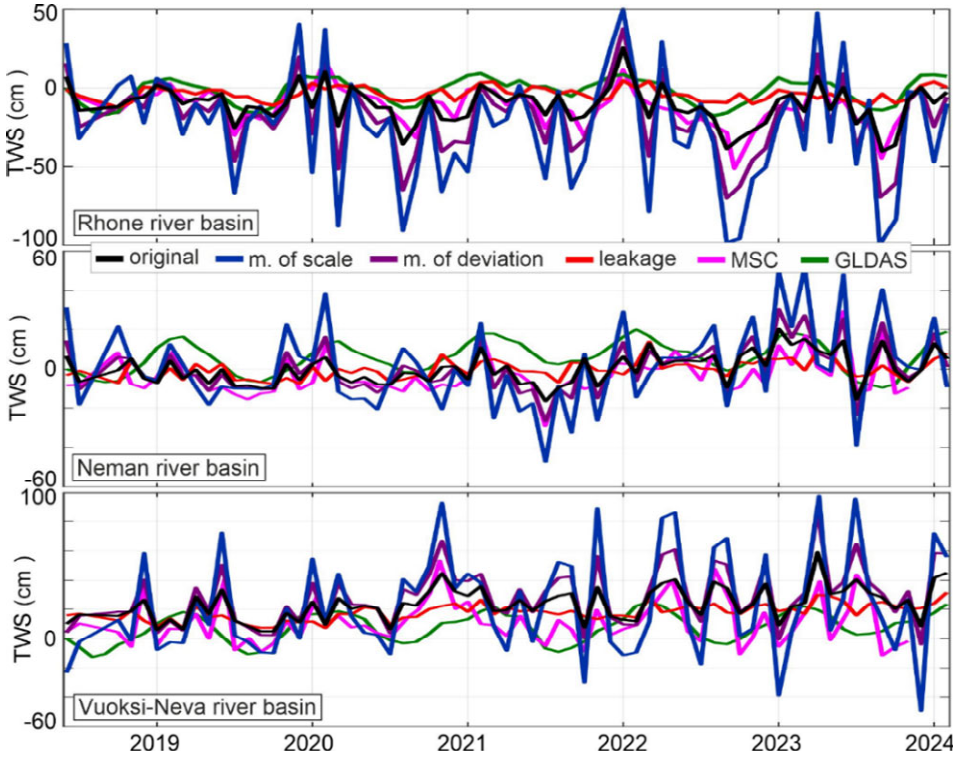

Notes: The true GRACE-FO leakage effect and TWS-derived for JPL mascon solution and for GLDAS Noah hydrological model are also presented. Values are given in cm.

They show significant inter-and annual changes, i.e., a linear trend above/below +/–3 cm/yr, or seasonal changes, i.e., (semi-)amplitudes greater than 5 cm. The selected regions reveal the largest discrepancies in TWS between original and both data-driven

filtering approaches as well. They also indicate a good inter-and annual temporal coherence of TWS signals between both GRACE-FO-type data and GLDAS. However, SHCs-derived TWS series show a greater signal variation than mascon solution. SHCs approaches also emphasise dry and wet period's more than original one. The first region, the Rhone river basin, covers about 98,500 km^2 area. It is located across France and Switzerland. The tributaries flowing from the Alps, the Jura, the Vosges, the Massif Central and the Cevennes indicate variable morphological, hydrological and ecological features that have affected the physical, chemical and biological qualities of the river in different ways. Flooding is here a regular occurrence, with varying intensity depending on the amount of natural rainfall over the year (Olivier et al., 2022). The significant rises and declines in TWS are captured by all GRACE-FO data between 2018–2024, especially for SHCs filtered by data-driven approaches. However, the higher fluctuations in monthly TWS series for GRACE-FO SHCs than for mascon (top series) are observed. For GRACE-FO period, Rhone basin shows increased groundwater scarcity caused by prolonged droughts and extensive irrigation that lead to more liquid precipitation, especially in winter, increasing streamflow maxima, and vegetation degradation (Ruiz-Villanueva et al., 2015). The effects are noticed as TWS increases of more than 50 cm for 2020, 2021/2022 and early 2023 periods, reflecting gains in water resources due to abundant rainfall in France and Switzerland areas. TWS increase from mid-2021 reflects severe flooding triggered by a storm complex relocated from UK, which has caused a several-fold increase in precipitation compared to regional averages (European State of the Climate, 2021). Changes in 2019 and 2023 reflect river flooding caused by extreme winter and spring rainfall events (e.g., Degeai et al., 2022). A steady TWS decline by almost 100 cm in 2020, 2022 and 2023 are consistent with the average decrease summer flow of Rhone river. This has already been noted by Viglione and Tamea (2023) as a decline in water levels of 10 cm relative to previous years. Although, compared to GRACE-type data, GLDAS fails to capture extreme events, however the seasonal signal is consistent over time. The true leakage signal oscillates within a 10 cm range, representing 6% to 15% of total TWS signal for original and both data-driven filtering approaches. Neman river basin rises in central Belarus and flows through Lithuania then forms the northern border of the Kaliningrad Oblast (Russia). Neman basin covers almost 90,000 km^2 area and is characterised by annual precipitation ranging from 520 to 800 mm. 40% of the river flow derives from surface meltwater, while water runoff accounts for about 20% of total runoff to the Baltic Proper subbasin (Gailiusis et al., 2001). Data-driven GRACE-FO signals are more consistent with mascon-derived TWS series than SHCs-derived TWS estimated using original filtering approach during non-drought/-flood periods (middle series). The observed delayed winter storms in northeastern Europe frequently lead to earlier spring snowmelt floods that are captured by GRACE-FO time series as TWS increases of up to 60 cm in 2019/2020 and 2022/2023 winter onwards. On the other hand, climate change leads to decreased runoff in summer over Neman basin, indicating, e.g., the lowest TWS values in 2021. Further significant TWS declines of about 80 cm are observed in 2023 reflecting dry conditions reported by SHCs European Environment Agency (official website), which identified the Neman basin region as the most drought impacted area; almost 35% of region was impacted by (extreme) dry conditions in 2023. The true leakage signal varies within ±10 cm, representing 10%–50% of total TWS signal according to the adopted filtering approaches. Last region, the Vuoksi-Neva river basin extends over 170,000 km^2 and contributed more than 40% of total flow into the Baltic Sea catchment area (HELCOM, 2021). The water resources are

strong dependent on rainfall and snowfall, leading to large seasonal changes in runoff and water levels. The strong climate-induced changes in TWS are captured by GRACE-FO series (bottom time series). For Vuoksi-Neva River, the recurring heavy rainfalls are registered since late 2020, indicating TWS variations in a range of 140 cm, for example, for winters in 2020, 2021, or springs/summers in 2022 and 2023. A steady decreases in GRACE-FO-derived TWS in 2021/2022 are associated with a severe lack of precipitation in the eastern parts of Europe. These weather conditions drove to one of the Europe's worst year in 2022 in the last 500 years (Garrido-Perez et al., 2024). As a consequence, the most European river basins underwent a drought exacerbated by heat waves in summer 2022, indicating very low soil moisture and river water levels (Bevacqua et al., 2024). It is reflected by decline in TWS values since June 2022. In 2023, Europe experienced further drought-like conditions amid heat waves, characterised by TWS declines of up to 80 cm for data-driven approaches. Analysis of magnitude of extreme events described shows that original approach mainly underestimates TWS changes; however, mascon smoothed series compared to both data-driven approaches. Nevertheless, all filtering approaches reveal a strong (> 0.7) correlation with mascons and near 0.2 weaker with GLDAS (Table 1). The estimated true leakage is significant and varies within ±20 cm, representing 10% to 40% of total TWS signal derived following original and data-driven filtering approaches.

5 Summary

The following research analyses the impact of spatial filtering method to GRACE-FO-derived TWS, i.e., magnitude of total TWS and true leakage signals over 24 European river basins. Traditional (original) Gaussian smoothing approach and two data-driven filtering approaches, i.e.

1 method of scale

2 method of deviation are applied.

They are based only on original gravity data. To detailed discussion, the three European regions, i.e., the Rhone, Neman and Vuoksi-Neva river basins are selected. Regions are characterised with significant variations in TWS.

For spatial analysis of intra-and annual TWS signals, mostly comparable trend signs and the magnitude of the (semi-)annual amplitudes over Europe for all datasets are observed. For GRACE-FO SHCs, there are changes in trend values by ±1–2 cm/yr and (semi-)annual amplitudes by up to 5 cm for river basins located in the western and the northeastern parts of Europe. The regions with extreme TWS values are spatially coherent with GRACE-FO mascon and are underestimated by GLDAS hydrological model, mostly in the western areas. The strongest spatial agreement with mascons as well as magnitude of RMS values is found for CSR SHCs and JPL SHCs filtered by Gaussian smoothing and method of deviation. For method of deviation, values are several cm larger than for original approach for river basins in Central Europe. It has been observed as well for mascons. For GLDAS, RMS values are overestimated for all river basins indicating values greater than 40 cm; however, there are also noticeably smaller RMS values for the central basins compared to the fringe European regions. Overall the largest differences between three used approaches in regions located on the belt coasts close to

the North Sea and the Baltic Sea, and river basins located in Turkey are found. The smallest variations are observed in Central Europe.

This study also shows that TWS leakage signal mainly represents at least 30% of total TWS signal for all three filtering methods and data processing centres. The highest contribution is found in the northern European river basins; a belt alongside the continental coast. The both data-driven approaches indicate less leakage than Gaussian smoothing approach. Moreover, GFZ SHCs is characterised with higher CCR values than others centres. The initial TWS leakage error parameter shows the highest uncertainty for original approach for all river basins; they are at least 2–3 times larger than for both data-driven approaches. The method of scale shows the smallest errors for all GRACE-FO data across Europe, not exceeding 15% of total TWS signal. The lowest values are noticed for CSR SHCs for all filtering approaches. On the other hand, the largest TWS signal reduction is obtained for method of deviation for CSR SHCs and GFZ SHCs for Europe. For JPL SHCs, the largest reduction for method of scale is observed. Signal reductions of mostly 30%–50% are found for all three GRACE-FO datasets using data-driven approaches compared to original one. The greatest values over 70% are noted for the Wisla, Danube, Dniestr, Northern Dvina, Volga and Don River basins for both filtering methods and data centres.

The regional analysis highlights the strong temporal coherence of monthly TWS estimated from GRACE-FO SHCs and mascon, and hydrological model during recorded periods of drought and flooding in European basins. However, the magnitude of TWS changes varies. This is indicated by an analysis of TWS changes during extreme events reported in the Rhone, Neman, and Vuoksi-Neva river basins. For the Rhone River, changes are related to increased winter streamflow maxima, reflecting TWS increases of more than 50 cm in 2020, 2021/2022 and early-2023. The changes are affected by winter and spring rainfalls or infrequent storms. TWS decreases are consistent with the average decrease summer river flow, leading to droughts in late 2020, and 2022, 2023. For Neman river, GRACE-FO TWS signals filtered by data-driven methods are more consistent with mascon-derived TWS than original SHCs TWS-derived for drought/flood-free periods. There is reduced runoff observed in summer and earlier spring snowmelt, resulting in, for example, 2021 drought, and 2019/2020 and 2022/2023 floods, respectively. Vuoksi-Neva River are highly dependent on rain and snowfall, leading to seasonal and intense changes in TWS signal. A heavy and severe rainfall deficit causes changes in TWS of 80–100 cm. The strongest water changes occur in 2020 and 2021 winters, or in spring and early summer in 2022 and 2023.

The obtained results highlight the impact of global warming on droughts are already underway in Europe, widespread, more dangerous and long-lasting, and drought risk might intensify with continuing human-induced warming in the future as well. Thus, the following analysis are a remarkable step toward improving the accuracy of the real (geo-)physical hydrological changes determination in the context of river basin studies, especially for small river basins dominating in Europe. The results also emphasise that implementing filtering methods based SHCs independent of external data (e.g., hydrological models) helps reduce the attenuated GRACE-FO TWS signal, proving better consistency of mascon-based results than original filtering approach. The analysis also provides important information on the condition and progress of more frequent meteorological, agricultural and hydrological droughts in Europe. The results also provide more relevant and updated information about climate change in river basins for operational decision-making.

Acknowledgements

This work was supported by the Military University of Technology, Faculty of Civil Engineering and Geodesy. GRACE-FO data in the form of spherical harmonic coefficients are available at International Centre for Global Earth Models (ICGEM) website (http://icgem.gfzpotsdam.de/). All low-degree coefficient replaced in GRACE data are available at https://podaac-tools.jpl.nasa.gov/drive/files/allData/gracefo. Gridded TWS changes for GRACE JPL mascon solution and GLDAS model are available at https://grace.jpl.nasa.gov/ and https://disc.gsfc.nasa.gov/, respectively. Maps are generated using the generic mapping tools software (Wessel et al., 2019).

Declarations

All authors declare that they have no conflicts of interest.

References

Barton, Y., Rivoire, P., Koh, J., Ali, M.S., Kopp, J. and Martius, O. (2022) 'On the temporal clustering of European extreme precipitation events and its relationship to persistent and transient large-scale atmospheric drivers', *Weather Climate Extreme*, Vol. 38, No. 100518, DOI: 10.1016/j.wace.2022.100518.

Bevacqua, E., Rakovec, O., Schumacher, D.L., Kumar, R., Thober, S., Samaniego, L., Seneviratne, S.I. and Zscheischler, J. (2024) 'Direct and lagged climate change effects intensified the 2022 European drought', *Nature Geoscience*, Vol. 17, pp.1100–1107, DOI: 10.1038/s41561-024-01559-2.

Cui, D., Liang, S. and Wang, D. (2021) 'Observed and projected changes in global climate zones based on Köppen climate classification', *WIREs Climate Change*, Vol. 12, No. 3, p.e701, DOI: 10.1002/wcc.701.

Dahle, C. (2024) *Release Notes for GFZ GRACE-FO Level-2 Products – version RL06.3 (Last Update, October 03, 2024)*, GFZ German Research Centre for Geosciences, Potsdam.

Degeai, J-P., Blanchemanche, P., Tavenne, L., Tillier, M., Bohbot, H., Devillers, B. and Dezileau, L. (2022) 'River flooding on the French Mediterranean coast and its relation to climate and land use change over the past two millennia', *Catena*, Vol. 219, No. 106623, DOI: 10.1016/j.catena.2022.106623.

European Drought Observatory (2018) *Drought in central-northern Europe – September 2018 (Tech. Rep.)*, JRC European Drought Observatory.

European Drought Observatory (2019) *Drought in Europe – August 2019 (Tech. Rep.)*, JRC European Drought Observatory.

European State of the Climate (2021) *Copernicus Climate Change Service*, Full report [online] http://www.climate.copernicus.eu/ESOTC/2021 (accessed 10 January 2025).

Gailiusis, B., Jablonskis, J. and Kovalenkoviene, M. (2001) *Lithuanian Rivers. Hydrography and Runoff*, Lithuanian Institute of Energy, Kaunas, p.57, p.136, p.149, p.240 (in Lithuanian).

Garrido-Perez, J.M., Vicente-Serrano, S.M., Barriopedro, D., García Ferrera, R., Trigo, R. and Beguería, S. (2024) 'Examining the outstanding Euro-Mediterranean drought of 2021–2022 and its historical context', *Journal of Hydrology*, Vol. 630, No. 130653, DOI: 10.1016/ j.jhydrol.2024.130653.

HELCOM (2021) 'Input of nutrients by the seven biggest rivers in the Baltic Sea region 1995-2017', *Baltic Sea Environment Proceedings No. 178*.

Ince, E.S., Barthelmes, F. and Reißland, S. (2019) 'ICGEM-15 years of successful collection and distribution of global gravitational models, associated services and future plans', *Earth System Science Data*, Vol. 11, pp.647–674, DOI: 10.5194/essd-11-647-2019.

Jekeli, C. (1981) *Alternative Methods to Smooth the Earth's Gravity Field*, Tech Rep 327, Department of Geodetic Science and Surveying, Ohio State Univ., Columbus, OH.

Kapica, J., Juracz, J., Canales, F.A., Bloomfield, H., Guezgouz, M., de Felice, M. and Kobus, Z. (2024) 'The potential impact of climate change on European renewable energy droughts', *Renewable and Sustainable Energy Reviews*, Part A, Vol. 189, p.117011, DOI: 10.1016/j.rser.2023.114011.

Khaki, M., Forootan, E., Kuhn, M., Awange, J., Longuevergne, L. and Wada, Y. (2018) 'Efficient basin scale filtering of GRACE satellite products', *Remote Sensing of Environment*, Vol. 204, pp.76–93, DOI: 10.1016/J.RSE.2017.10.040.

Kim, H., Yeh, P.J-F., Oki, T. and Kanae, S. (2009) 'Role of rivers in the seasonal variations of terrestrial water storage over global basins', *Geophysical Research Letters*, Vol. 36, No. 17, DOI: 10.1029/2009GL039006.

Kim, J. and Lee, S.W. (2009) 'Flight performance analysis of GRACE K-band ranging instrument with simulation data', *Acta Astronautica*, Vol. 65, Nos. 11–12, pp.1571–1581, DOI: 10.1016/j.actaastro.2009.04.010.

Knutzen, F., Averbeck, P., Barrasso, C. et al. (2025) 'Impacts on and damage to European forests from the 2018–2022 heat and drought events', *Natural Hazards and Earth System Sciences*, Vol. 25, No. 1, pp.77–117, DOI: 10.5194/nhess-25-77-2025.

Landerer, F.W. and Swenson, S.C. (2012) 'Accuracy of scaled GRACE terrestrial water storage estimates', *Water Resources Research*, Vol. 48, No. 4, DOI: 10.1029/2011WR011453.

Landerer, F.W., Flechtner, F.M., Save, H., Webb, F.H., Bandikova, T., Bertiger, W.I., Bettadpur, S.V., Byun, S.H., Dahle, C., Doblaw, H., Fahnestock, E., Harvey, N., Kang, Z., Kruizinga, G.L.H., Loomis, B.D., McCullough, C., Murbock, M., Nagel, P., Paik, M., Pie, N., Poole, S., Strekalov, D., Tamisea, M.E., Wang, F., Watkins, M.M., Wen, H-Y., Wiese, D.N. and Yuan, D-N. (2020) 'Extending the global mass change data record: GRACE follow-on instrument and science data performance', *Geophysical Research Letters*, Vol. 47, No. e2020GL088306, DOI: 10.1029/2020GL088306.

Lehmkuhl, F., Schüttrumpf, H., Schwarzbauer, J., Brüll, C., Dietze, M., Letmathe, P., Völker, C. and Hollert, H. (2022) 'Assessment of the 2021 summer flood in Central Europe', *Environment Sciences Europe*, Vol. 34, No. 107, DOI: 10.1186/s12302-022-00685-1.

Lenczuk, A., Leszczuk, G., Klos, A. and Bogusz, J. (2020) 'Comparing variance of signal contained in the most recent GRACE solutions', *Geodesy and Cartography*, Vol. 69, No. 1, pp.19–37, DOI: 10.24425/gac.2020.131084.

Li, J., Chen, J., Li, Z., Wang, S-Y. and Hu, X. (2017) 'Ellipsoidal correction in GRACE surface mass change estimation', *Journal of Geophysical Research: Solid Earth*, Vol. 122, pp.9437–9460, DOI: 10.1002/2017JB014033.

McCullough, C.M., Fahnestock, E.G., Ellmer, M., Wiese, D.N. and Yaun, D-N. (2024) *JPL Level-2 GRACE-FO Products – Release Notes Version 6.3 (Last Update, August 20, 2024)*, Jet Propulsion Laboratory, California Institute of Technology.

Olivier, J.M., Carrel, G., Lamouroux, N., Dole-Oliver, M-J., Malard, F., Bravard, J-P., Piegay, H., Castella, E. and Barthelemy, C. (2022) 'Rivers of Europe', in Tockner, K., Zarflm, C. and Robinson, C.T. (Eds.), Elsevier, Radarweg 29, PO Box 211, 1000 AE Amsterdam, Netherlands, DOI: 10.1016/B978-0-08-102612-0.00011-0.

Peltier, W.R., Argus, D.F. and Drummond, R. (2018) 'Comment on 'an assessment of the ICE-6G_C (VM5a) glacial isostatic adjustment model by Purcell et al.', *Journal of Geophysical Research: Solid Earth*, Vol. 123, pp.2019–2028, DOI: 10.1002/2016JB01384.

Rakovec, O., Samaniego, L., Hari, V., Markonis, Y., Moravec, V., Thober, S., Hanel, M. and Kumar, R. (2022) 'The 2018–2020 multi-year drought sets a new benchmark in Europe', *Earth's Future*, Vol. 10, No. 3, p.e2021EF002394, DOI: 10.1029/2021EF002394.

Ries, J., Bettadpur, S., Eanes, R., Kang, Z., Ko, U-D., McCullough, C., Nagel, P., Pie, N., Poole, S., Richter, T., Save, H. and Tapley, B. (2016) 'The combined gravity model GGM05C', *GFZ Data Services*, DOI: 10.5880/icgem.2016.002.

Rodell, M. and Beaudoing, K.H. (2003) *GLDAS NOAH Land Surface Model L4 Monthly 1.0×1.0 Degree, Version 001*, Technical Report, Goddard Earth Sciences Data and Information Services Center (GESDISC), Greenbelt 2003.

Rodell, M., Famiglietti, J.S., Wiese, D.N., Reager, J.T., Beaudoing, H.K., Landerer, F.W. and Lo, M-H. (2018) 'Emerging trends in global freshwater availability', *Nature*, Vol. 557, pp.651–659, DOI: 10.1038/s41586-018-0123-1.

Rodell, M., Houser, P.R., Jambor, U., Gottschlack, J., Mitchell, K., Meng, C-J., Arsenault, K., Cosgrove, B., Radakovich, J., Bosilovich, M., Entin, J.K., Walker, J.P., Lohmann, D., Toll, D. (2004) 'The global land data assimilation system', *Bulletin of the American Meteorological Society*, Vol. 85, No. 3, pp.381–394, DOI: 10.1175/BAMS-85-3-381.

Ruiz-Villanueva, V., Stoffel, M., Bussi, G., Francés, F., Bréthaut, C. (2015) 'Climate change impacts on discharges of the Rhone River in Lyon by the end of the twenty-first century: model results and implications', *Regional Environmental Change*, Vol. 15, pp.505–515, DOI: 10.1007/s10113-014-0707-8.

Save, H. (2024) *Release Notes for GRACE-FO L-2 Products – Version UTCSR RL-06.3 (Last Update, October 09, 2024)*, Center for Space Research, The University of Texas at Austin.

Save, H., Bettadpur, S. and Tapley, B.D. (2016) 'High-resolution CSR GRACE RL05 mascons', *Journal of Geophysical Research: Solid Earth*, Vol. 121, No. 10, pp.7547–7569, DOI: 10.1002/2016jb013007.

Schmied, H.M., Caceres, D., Eisner, S., Flörke, M., Herbert, C., Niemann, C., Peiris, T.A., Popat, E., Portmann, F.T., Reinecke, R., Schumacher, M., Shadkam, S., Telteu, C-E., Trautmann, T. and Döll, P. (2021) 'The global water resources and use model WaterGAP v2.2d: model description and evaluation', *Geoscience Model Development*, Vol. 14, pp.1037–1079, DOI: 10.5194/gmd-14-1037-2021.

Sun, Y., Riva, R. and Ditmar, P.(2016) 'Optimizing estimates of annual variations and trends in geocenter motion and J2 from a combination of GRACE data and geophysical models', *Journal of Geophysical Research: Solid Earth*, Vol. 121, DOI: 10.1002/2016JB013073.

Tapley, B.D., Bettadpur, S., Watkins, M. and Reigber, C. (2004) 'The gravity recovery and climate experiment: mission overview and early results', *Geophysical Research Letters*, Vol. 31, No. L09607, DOI: 10.1029/2004GL019920.

Toreti, A., Belward, A., Perez-Dominguez, I., Naumann, G., Luterbacher, J., Cronie, O., Seguini, L., Manfron, G., Lopez-Lozano, R., Baruth, B., van den Berg, M., Dentener, F., Ceglar, A., Chatzopoulos, T. and Zampieri, M. (2019) 'The exceptional 2018 European water seesaw calls for action on adaptation', *Earth's Future*, Vol. 7, pp.652–663, DOI: 10.1029/2019EF001170.

Viglione, A. and Tamea, S. (2023) 'A comparison analysis: the 2022 drought on the Rhone and the Po basins', *Politecnico di Torino, Corso di laurea magistrale in Ingegneria Per L'Ambiente E Il Territorio*.

Vishwakarma, B.D., Devaraju, B. and Sneeuw, N. (2016) 'Minimizing the effects of filtering on catchment scale GRACE solutions', *Water Resources Research*, Vol. 52, No. 8, pp.5868–5890, DOI: 10.1002/2016WR018960.

Vishwakarma, B.D., Horwath, M., Devaraju, B., Groh, A. and Sneeuw, N. (2017) 'A data-driven approach for repairing the hydrological catchment signal damage due to filtering of GRACE products', *Water Resources Research*, Vol. 53, No. 11, pp.9824–9844, DOI: 10.1002/2017WR021150.

Wahr, J., Molenaar, M. and Bryan, F. (1998) 'Time variability of the Earth's gravity field: hydrological and oceanic effects and their possible detection using GRACE', *Journal of Geophysical Research: Solid Earth*, Vol. 103, pp.30205–30229, DOI: 10.1029/98JB02844.

Wessel, P., Luis, J.F., Uieda, L., Scharroo, R., Wobbe, F., Smith, W.H.F. and Tian, D. (2019) 'The generic mapping tools version 6', *Geochemistry, Geophysics, Geosystems*, Vol. 20, No. 11, pp.5556–5564, DOI: 10.1029/2019GC008515.

Wiese, D.N., Landerer, F.W. and Watkins, M.M. (2016) 'Quantifying and reducing leakage errors in the JPL RL05M GRACE mascon solution', *Water Resources Research*, Vol. 52, No. 9, pp.7490–7502, DOI: 10.1002/2016WR019344.

Xanke, J. and Liesch, T. (2022) 'Quantification and possible causes of declining groundwater resources in the Euro-Mediterranean region from 2003 to 2020', *Hydrogeology Journal*, Vol. 30, No. 2, pp.379–400, DOI: 10.1007/s10040-021-02448-3.

Appendix

Table A1 Summary of the total river area, climate zone and major hydrological events by which the rivers were affected

	River basin	*Area (1,000 km²)*	*Climate zone (Cui et al., 2021)*	*Hydrological event (year)*
1	Douro	97.3	Cold semi-arid	D: 2018 winter, 2021/2022, 2023 autumn W: 2018 spring
2	Ebro	88.5	Cold semi-arid	D: 2022–2023 W: 2020–2021
3	Rhone	98.5	Temperate oceanic	W: 2020, 2021/2022, 2023 D: 2022 summer, 2023
4	Po	74.0	Temperate oceanic	D: 2022 summer, 2023 W: 2019–2020
5	Loire	117.0	Temperate oceanic	D: 2022 summer, 2023 W: 2019–2020
6	Seine	78.6	Temperate oceanic	D: 2022 summer, 2023 spring W: 2020–2021
7	Rhine	185.0	Temperate oceanic	D: 2018 winter, 2022 and 2023 summers W: 2020–2021
8	Elbe	148.3	Warm-summer humid continental	D: 2018 and 2019 summers, 2022 W: 2020–2021
9	Oder	118.8	Warm-summer humid continental	D: 2018 and 2019 summers, 2022 W: 2020–2021
10	Wisla	169.0	Warm-summer humid continental	D: 2018 and 2019 summers, 2022 W: 2020–2021
11	Danube	817.0	Warm-summer humid continental	D: 2018 and 2019 summers, 2022 W: -
12	Dniestr	72.1	Warm-summer humid continental	D: 2018 and 2019 summers, 2022 W: 2020 summer

Notes: The assignment to climate zones was based on the dominant % of the river basin area. For hydrological events, years of major dry (D) and wet (W) events are presented.

Table A1 Summary of the total river area, climate zone and major hydrological events by which the rivers were affected (continued)

	River basin	*Area (1,000 km^2)*	*Climate zone (Cui et al., 2021)*	*Hydrological event (year)*
13	Neman	90.0	Warm-summer humid continental	D: 2021 summer, 2023
				W: 2019/2020, 2022/2023
14	Western Dvina	88.0	Warm-summer humid continental	D: -
				W: -
15	Narva	56.2	Warm-summer humid continental	D: 2018–2020
				W: -
16	Vuoksi-Neva	345.0	Subarctic	D: 2021/2022, 2022 summer
				W: 2020 and 2021 winters, 2022 and 2023 springs/summers
17	Northern Dvina	357.0	Subarctic	D: 2018 and 2019 summers
				W: 2020–2021
18	Volga	1,360.0	Warm-summer humid continental	D: 2018 and 2019 summers, 2022 autumn
				W: 2020–2021
19	Don	425.6	Warm-summer humid continental	D: 2018 and 2019 summers, 2022 autumn
				W: 2020–2021
20	Kura-Ozero Sevan	188.0	Warm-summer humid continental/cold semi-arid	D: 2018, 2019 and 2020 summers
				W: 2020 autumn
21	Tigris-Euphrates	875.0	Hot desert	D: 2018 and 2019 summers, 2022–2023
				W: -
22	Kizilirmak	78.0	Cold semi-arid	D: 2018 and 2019 summers, 2022–2023
				W: -
23	Sakarya	85.0	Cold semi-arid	D: 2018 and 2019 summers
				W: -
24	Dniepr	516.3	Warm-summer humid continental	D: 2018 and 2019 summers
				W: 2023 summer

Notes: The assignment to climate zones was based on the dominant % of the river basin area. For hydrological events, years of major dry (D) and wet (W) events are presented.

Table A2 The statistics of the linear trend (cm/yr) estimated within European river basins for average GRACE-FO TWS changes derived for SHC provided by CSR, GFZ, JPL and mascon solution (MSC), and GLDAS hydrological model

	River basin	*CSR*			*GFZ*			*JPL*			*MSC JPL*	*GLDAS*
		Original	*Method of scale*	*Method of deviation*	*Original*	*Method of scale*	*Method of deviation*	*Original*	*Method of scale*	*Method of deviation*		
1	Douro	0.5	2.3	1.2	0.6	1.7	1.1	1.8	7.1	4.1	0.3	–0.2
2	Ebro	–1.3	–4.4	–2.5	–0.8	–0.4	–1.3	–1.8	–5.0	–3.6	–0.7	–2.1
3	Rhone	–1.3	–3.7	–2.5	–2.1	–4.6	–4.8	–2.2	–7.2	–5.3	–2.5	0.2
4	Po	–1.4	–1.8	–2.0	–2.5	–3.2	–4.3	–0.4	1.3	–0.1	–2.7	0.1
5	Loire	0.4	1.8	0.9	0.9	4.6	2.2	0.8	4.3	2.0	–0.3	–0.1
6	Seine	0.7	1.0	1.0	1.2	4.7	2.6	0.1	–0.8	–0.2	–0.4	0.3
7	Rhine	0.5	1.5	0.9	–0.6	0.1	–0.5	1.8	5.2	3.6	–0.9	0.8
8	Elbe	0.6	1.0	0.9	0.0	–1.4	–0.4	–0.1	–1.3	–0.6	0.3	1.2
9	Oder	0.8	0.7	0.8	2.7	6.8	5.0	0.3	0.2	0.3	–0.3	1.5
10	Wisla	1.2	1.6	1.4	–0.3	–1.6	–0.8	1.2	1.9	1.5	–0.4	1.0
11	Danube	–0.2	–0.4	–0.4	–0.4	–0.4	–0.4	–0.5	–0.8	–0.8	–0.7	1.1
12	Dniestr	–0.3	–1.8	–0.6	–0.4	1.9	0.0	0.1	0.4	0.2	–1.6	0.7
13	Neman	1.9	2.3	2.1	0.8	2.1	1.6	2.5	4.5	3.5	0.5	0.7
14	Western Dvina	1.3	–0.6	0.9	1.0	0.8	1.1	1.2	–1.1	0.9	0.9	1.3
15	Narva	2.8	7.5	5.2	2.4	8.5	6.0	1.8	1.8	2.9	3.2	1.0
16	Vuoksi-Neva	3.4	4.5	4.5	4.1	10.4	7.9	2.8	1.1	3.3	2.7	1.7
17	Northern Dvina	–0.3	–0.3	–0.4	–0.7	–1.0	–1.0	–0.2	0.0	–0.1	–1.4	0.0
18	Volga	0.0	–0.1	0.0	–0.2	–0.4	–0.3	0.1	0.0	0.1	–1.6	1.5
19	Don	1.8	2.4	2.2	1.3	1.4	1.4	1.6	2.1	1.7	1.0	1.7
20	Kura-Ozero Sevan	–3.5	–2.6	–3.0	–2.8	–1.8	–2.4	–3.0	–1.4	–2.4	–3.6	1.4
21	Tigris-Euphrates	–3.5	–4.0	–4.0	–3.5	–6.1	–4.9	–3.6	–5.7	–4.8	–3.1	–1.6
22	Kizilirmak	–0.8	–0.4	–0.8	2.9	10.3	7.9	0.0	4.9	1.2	–2.2	0.8
23	Sakarya	–1.1	–0.7	–1.4	–4.5	–9.7	–9.2	–2.3	–7.0	–5.0	–2.3	0.1
24	Dnieprr	1.3	1.5	1.4	0.7	0.9	0.9	1.2	1.4	1.3	–1.1	1.9

Note: GRACE-FO SHC signals are up to degree and order 96, and are filtered with Gaussian smoothing with radius equal to 400 km (original) and using two data-driven approaches, i.e., method of scale and method of deviation.

Table A3 The statistics of the amplitude of the annual oscillation (cm) estimated within European river basins for average GRACE-FO TWS changes derived for SHC provided by CSR, GFZ, JPL and mascon solution (MSC), and GLDAS hydrological model

	River basin	*CSR*			*GFZ*			*JPL*			*MSC JPL*	*GLDAS*
		Original	*Method of scale*	*Method of deviation*	*Original*	*Method of scale*	*Method of deviation*	*Original*	*Method of scale*	*Method of deviation*		
1	Douro	4.8	5.5	6.8	3.9	11.0	6.9	4.2	14.7	10.3	5.0	12.0
2	Ebro	3.5	5.9	4.7	7.4	15.3	14.7	9.5	18.1	13.0	5.1	6.0
3	Rhone	9.3	13.3	15.3	12.0	14.9	15.2	6.9	14.0	14.4	7.1	9.7
4	Po	3.9	6.4	5.2	2.5	8.9	4.5	4.9	9.3	8.5	8.1	7.7
5	Loire	7.2	7.2	8.1	4.0	7.9	1.4	8.8	14.8	11.4	7.5	10.9
6	Seine	8.9	12.8	12.3	10.1	19.8	16.8	7.3	9.6	11.2	8.7	10.7
7	Rhine	5.1	3.8	5.1	4.6	5.9	5.3	5.5	5.5	6.7	10.1	11.1
8	Elbe	4.6	5.6	5.8	6.3	12.1	10.3	5.0	5.3	6.8	4.6	9.8
9	Oder	4.7	5.5	5.7	4.4	6.6	5.1	4.8	4.8	6.3	5.0	9.1
10	Wisla	3.7	2.5	3.4	5.2	7.3	6.8	5.7	8.0	7.0	5.3	7.5
11	Danube	5.0	5.1	4.9	5.0	4.8	4.8	5.3	5.1	5.3	9.1	6.2
12	Dniestr	4.2	5.9	4.7	2.9	3.5	2.4	4.1	6.2	4.4	5.3	8.8
13	Neman	4.2	6.8	5.0	1.1	10.5	3.2	5.3	8.8	6.6	5.0	10.0
14	Western Dvina	3.1	2.6	2.3	4.5	7.0	5.7	4.5	8.1	5.4	5.1	11.8
15	Narva	5.5	16.6	10.6	2.1	5.6	4.1	5.3	13.1	10.4	4.4	12.2
16	Vuoksi-Neva	2.8	3.7	3.6	6.0	24.1	13.6	4.2	16.8	8.0	7.0	12.5
17	Northern Dvina	5.0	4.4	4.4	3.9	1.0	2.2	4.4	2.8	2.9	8.5	14.4
18	Volga	6.2	6.5	6.5	6.3	6.5	6.6	6.8	6.9	7.1	8.4	15.5
19	Don	6.5	7.4	7.2	6.5	7.5	7.5	6.0	4.9	6.1	9.6	14.1
20	Kura-Ozero Sevan	3.6	1.9	2.7	3.2	5.5	3.4	4.9	5.8	5.3	4.0	5.4
21	Tigris-Euphrates	10.0	14.3	12.8	8.3	7.7	9.8	10.0	15.8	13.7	7.5	4.3
22	Kizilirmak	5.9	7.9	6.5	4.8	9.4	8.0	5.8	2.6	5.3	12.5	10.2
23	Sakarya	9.5	21.4	15.1	8.6	17.6	15.3	7.4	12.3	13.3	7.4	9.2
24	Dniepr	5.3	5.7	5.9	5.1	5.5	5.7	5.0	4.2	4.7	8.7	6.1

Note: GRACE-FO SHC signals are up to degree and order 96, and are filtered with Gaussian smoothing with radius equal to 400 km (original) and using two data-driven approaches, i.e., method of scale and method of deviation.

Table A4 The statistics of the amplitude of the semiannual oscillation (cm) estimated within European river basins for average GRACE-FO TWS changes derived for SHC provided by CSR, GFZ, JPL and mascon solution (MSC), and GLDAS hydrological model

	River basin	*CSR*			*GFZ*			*JPL*			*MSC JPL*	*GLDAS*
		Original	*Method of scale*	*Method of deviation*	*Original*	*Method of scale*	*Method of deviation*	*Original*	*Method of scale*	*Method of deviation*		
1	Douro	2.4	2.8	3.3	2.4	17.0	7.5	3.8	20.1	9.7	2.6	2.9
2	Ebro	2.5	0.8	2.9	7.5	12.1	11.5	5.0	13.6	9.7	2.6	1.0
3	Rhone	4.3	13.7	8.5	5.3	11.3	10.9	5.6	11.9	13.2	2.2	2.9
4	Po	3.3	10.5	6.0	2.0	9.9	5.2	1.2	7.5	3.0	2.0	2.4
5	Loire	1.8	2.1	1.5	3.0	9.5	7.3	1.3	8.5	3.3	1.7	1.1
6	Seine	2.2	4.9	3.4	4.1	10.6	8.5	1.2	9.2	3.7	1.4	0.4
7	Rhine	3.2	6.7	4.9	2.8	10.8	6.6	1.9	2.3	2.5	1.9	0.8
8	Elbe	2.4	4.5	3.6	4.9	11.1	9.6	4.0	11.0	7.9	1.1	0.1
9	Oder	1.7	2.6	2.0	0.9	6.8	2.9	0.7	3.7	0.9	1.1	0.5
10	Wisla	0.8	1.3	1.0	2.6	5.6	4.2	0.8	3.7	1.9	0.6	0.5
11	Danube	0.8	0.8	0.8	0.8	1.0	1.0	0.4	0.6	0.7	1.8	0.6
12	Dniestr	0.9	3.5	1.5	2.8	11.9	5.0	2.8	13.1	5.0	0.6	0.2
13	Neman	0.5	3.0	1.0	3.1	10.8	8.1	0.8	3.7	1.4	0.8	0.9
14	Western Dvina	1.8	5.0	2.4	3.0	10.2	4.9	1.8	6.0	2.8	0.6	0.5
15	Narva	3.1	9.7	6.0	5.4	12.7	13.4	3.5	12.1	7.7	0.5	0.4
16	Vuoksi-Neva	2.4	4.7	3.4	4.9	10.7	9.8	3.0	11.6	5.9	1.0	2.1
17	Northern Dvina	3.1	3.4	3.0	3.8	4.1	4.0	2.6	1.9	2.1	2.7	2.1
18	Volga	2.5	2.6	2.6	2.8	3.2	3.2	2.6	3.1	2.9	0.6	1.3
19	Don	2.4	3.2	3.0	2.4	3.2	2.7	2.0	3.0	2.3	0.7	0.5
20	Kura-Ozero Sevan	1.7	3.4	2.4	2.0	4.8	3.2	2.0	6.8	4.1	1.0	1.0
21	Tigris-Euphrates	0.8	1.2	0.2	3.0	9.6	5.8	0.8	6.4	2.8	1.6	0.6
22	Kizilirmak	0.8	5.8	2.1	4.1	11.8	10.4	1.2	10.2	3.5	1.3	0.4
23	Sakarya	1.4	4.3	2.5	5.4	12.5	11.1	3.2	10.2	7.1	1.2	1.4
24	Dniepr	1.2	1.2	1.2	1.7	3.0	2.8	0.6	0.8	0.9	0.6	0.6

Note: GRACE-FO SHC signals are up to degree and order 96, and are filtered with Gaussian smoothing with radius equal to 400 km (original) and using two data-driven approaches, i.e., method of scale and method of deviation.

Table A5 The statistics of the RMS (cm) estimated within European river basins for average GRACE-FO TWS changes derived for SHC provided by CSR, GFZ, JPL and mascon solution (MSC), and GLDAS hydrological model

	River basin	*CSR*			*GFZ*			*JPL*			*MSC JPL*	*GLDAS*
		Original	*Method of scale*	*Method of deviation*	*Original*	*Method of scale*	*Method of deviation*	*Original*	*Method of scale*	*Method of deviation*		
1	Douro	9.9	30.5	18.9	11.6	60.7	37.1	10.4	57.2	32.3	5.5	48.9
2	Ebro	10.8	36.2	20.4	12.0	74.9	49.4	14.6	62.2	37.0	6.1	43.1
3	Rhone	16.3	44.4	29.9	13.3	86.8	84.2	19.5	67.7	46.9	13.3	52.3
4	Po	12.3	34.7	21.3	20.4	77.9	44.8	15.9	54.1	33.1	17.0	71.2
5	Loire	9.2	19.4	12.8	22.3	46.6	30.7	10.1	26.6	15.7	10.6	45.5
6	Seine	14.8	43.1	25.3	26.8	65.5	44.5	18.8	67.4	39.3	15.0	48.2
7	Rhine	10.0	20.3	14.3	25.3	40.9	34.5	12.3	30.9	21.4	15.5	51.9
8	Elbe	11.3	24.3	17.9	26.7	46.6	38.5	15.4	39.9	29.4	8.7	53.1
9	Oder	9.5	22.8	14.9	38.5	59.9	56.7	13.7	41.8	27.2	8.2	51.2
10	Wisla	8.8	14.3	11.2	27.3	30.4	31.5	10.1	21.0	14.6	10.8	40.1
11	Danube	7.5	7.7	7.6	17.4	17.5	17.5	8.1	8.5	8.7	11.9	41.8
12	Dniestr	12.2	21.4	14.9	17.5	30.3	20.9	14.1	29.4	18.2	17.0	44.9
13	Neman	7.8	20.4	11.6	38.2	61.3	59.9	12.5	39.4	21.9	7.8	55.9
14	Western Dvina	6.6	17.0	7.9	42.5	60.0	52.0	8.9	29.0	13.4	4.6	56.4
15	Narva	12.5	43.3	24.7	54.5	104.9	102.2	19.1	79.9	44.6	6.5	56.3
16	Vuoksi-Neva	26.2	42.0	34.6	81.1	104.4	107.9	26.4	57.0	39.5	6.4	58.4
17	Northern Dvina	7.4	7.8	7.1	57.5	52.7	53.5	7.7	10.0	8.2	7.6	73.4
18	Volga	7.0	7.4	7.4	43.1	43.2	44.2	7.1	7.5	7.5	13.5	60.7
19	Don	9.7	11.1	10.8	27.9	30.4	32.0	9.7	10.9	10.7	16.7	53.4
20	Kura-Ozero Sevan	22.1	17.4	18.7	12.4	21.8	13.9	22.3	21.3	20.9	32.5	51.9
21	Tigris-Euphrates	13.4	23.7	17.6	15.3	36.4	24.2	16.2	33.0	24.2	15.4	58.2
22	Kizilirmak	14.8	39.6	22.4	20.6	86.2	49.2	15.2	60.6	27.4	14.3	47.1
23	Sakarya	13.5	41.3	23.1	23.1	109.5	54.8	23.1	92.0	54.4	10.2	49.1
24	Dnieprr	12.2	13.8	13.7	23.7	23.4	25.7	12.5	14.2	14.2	20.6	56.8

Note: GRACE-FO SHC signals are up to degree and order 96, and are filtered with Gaussian smoothing with radius equal to 400 km (original) and using two data-driven approaches, i.e., method of scale and method of deviation.